Dependence of Pit Formation in Hard Tissue of Human Teeth on Free Electron Laser Pulse Structures

Yuma Sasamoto[1], Tetsuro Kono*[2], and Takeshi Sakai [3]

[1] Nihon University Graduate School of Dentistry at Matsudo, Histology, Cytology and Developmental Anatomy, Matsudo, Chiba 271-8587, Japan

[2] Department of Histology, Nihon University School of Dentistry at Matsudo, Matsudo, Chiba 271-8587, Japan

[3] Laboratory for Electron Beam Research and Application (LEBRA), Institute of Quantum Science, Funabashi Campus of College of Science and Technology, Nihon University, Funabashi, Chiba 274-8501, Japan

* Correspondence to Tetsuro Kono

e-mail: kono.tetsuro@nihon-u.ac.jp; Tel. & Fax: +81-47-360-9323

Address: Department of Histology, Nihon University School of Dentistry at Matsudo, 2-870-1, Sakaecho-Nishi, Matsudo, Chiba 271-8587, Japan

Abstract:

The purpose of this study was to compare and clarify the differences in pit formation between two modes of free-electron laser (FEL) irradiation with different beam currents and pulse structures and how the effects of these modes vary with the tissue structure of human teeth.

FEL irradiation using the full-bunch mode (Fm) and burst mode (Bm). The beam current was carried out at 200 mA for Fm and 2 A for Bm. The micro-pulse interval within the macro-pulse structure was 350 ps for Fm and 22.4 ns for Bm. The wavelength of the FEL was adjusted to 2.94 μm, and macro-pulse energy was adjusted to 6.0 mJ/macro-pulse by polarizing plate. The macro-pulse irradiation was set to 1 or 5 times for both modes.

As the number of macro-pulse irradiations increased, the pits became deeper in Fm than in Bm, regardless of the site on the tooth. On the other hand, the bulge height was lower for Bm than for Fm, regardless of the site on the tooth or the number of macro-pulse irradiations. No scorch marks were observed in the pits for either mode.

It was concluded that the differences in the pit including bulge formation were the macro-pulse structure between Fm and Bm. The intensity of the FEL irradiation caused plasma evaporation in the tooth hard tissue, and the tooth substance was ablated before thermal conduction occurred. The relation with the thermal relaxation time also confirmed that pits were formed without visible scorch marks.

Introduction

The fields in which lasers are applied are extremely broad and include precision measurements, product machining, optical telecommunications, information processing, and clinical medicine. Even in dentistry, laser irradiation is widely used for surgical applications such as cutting hard tissue, incision, excision, and coagulation of soft tissue, as well as for diagnosis of dental caries, pain relief, and promotion of wound healing (1, 2). In Japan, procedures such as caries treatment and dental scaling using lasers have recently become covered by medical insurance (3), and there is great anticipation for the practical use of lasers.

Research into lasers began with the theory of stimulated emission published by Einstein in 1916 (4). Among the many experiments that were subsequently conducted, Maiman (5), who was a scientist at Hughes Aircraft Company, successfully developed a ruby laser that emitted a crimson-red beam from a ruby crystal in 1960, and a year later, the He-Ne laser was developed for use in the field of medicine, which opened the door to the development of medical applications. Research into dental lasers began at the beginning of 1964 (6). When treatment of hard tissue using Er:YAG lasers became possible in the mid-1990s, treatment of caries and dental scaling began to be performed, and today this has advanced to the point of scraping bone, and even more progress is being made in research and development (7).

Lasers differ from conventional light sources and offer excellent properties such as monochromaticity, directivity, convergence, and coherence. However, commercial lasers

suffer from a limited wavelength range. Attention has therefore shifted to free-electron lasers (FELs), which use a high-energy electron beam generated by an accelerator. They have the unique characteristic of variable wavelength, from the far infrared to soft X-ray regions, which cannot be obtained with conventional lasers (8). FELs generated a wiggling motion in an electron beam that has a speed close to that of light (electron bunching) by using a periodic magnetic field produced by a device called an undulator, and they generate a coherent electromagnetic wave (undulator radiation) by the resonant interaction with the electromagnetic field. The wavelength of an FEL can be easily tuned by changing the energy of the electron beam and the strength of the magnetic field (undulator gap length). FELs generated in FEL systems using RF linear electron accelerators have a characteristic macro-pulse structure composed of micro-pulses (9). The Laboratory for Electron Beam Research and Application in Nihon University (LEBRA) has been performing research into the dental use of FELs, including the wavelength dependence of laser effects. Although drilling a hole in teeth was previously performed using an FEL, this was carried out with a full-bunch-mode (Fm) electron beam (10,11). LEBRA has been working on improving the FEL oscillator device, and it is now possible to use a high-current electron beam operating mode that was not previously possible. For joint-use experiments, LEBRA is currently offering both Fm with a macro-pulse beam current of around 200 mA, and burst mode (Bm) which has a peak beam current of around 2 A, an order of magnitude higher than the current in Fm.

In the present study, we aimed to compare and clarify the differences in Pit formation between two modes of FEL irradiation with different beam currents and pulse structures, and how the effects of these modes vary with the tissue structure of human teeth.

Materials and Methods

Sample preparation

The stocked 15 human third molars were used. All of the teeth used were selected from those with no attrition on the cusp and teeth with complete roots. The use of human teeth in the present study was approved by the Ethics Committee of Nihon University (No. EC22-17-015-1).

The teeth were cut using a diamond saw (IsoMet, Buehler Co. Ltd., Lake Bluff, IL, USA) in the longitudinally parallel to the buccolingual tooth axis. Sliced sections were used as samples with a thickness of approximately 0.5 mm and polished using a grinding stone up to grit #3,000 so that the surface was parallel to the sample stage. The polished sections were cleaned ultrasonically before use in the studies.

Sliced sections of human teeth were attached to slide glass using a transparent adhesive (Super-Clear Bond, Shinto Sangyo Co., Ltd., Osaka, Japan) (**Figure 1**). In a preliminary study, 60 sections prepared from 15 teeth were preliminarily FEL irradiated to set conditions. Afterward, one case was presented, for which the irradiation conditions were correctly applied across the entire procedure.

LEBRA-FEL system

The FEL equipment at the LEBRA was used in the present study. The electron linear

accelerator is composed of a triode direct current (DC) electron gun with an accelerating frequency of 2,856 MHz at -100 kV, a pre-buncher, a buncher, and three 4-m acceleration tubes. This is a simple system that does not use a radio frequency (RF) electron gun, sub-harmonic buncher, or superconducting acceleration system. **Figure 2** shows a schematic diagram of the LEBRA accelerator beamline, and **Table 1** shows the specifications of the linear accelerator.

The DC electron gun incorporates a high-speed grid pulser with a full width at half maximum of 600 ps (Kentech Instruments Ltd., Wallingford, U.K.) and a regular grid pulser. In addition to regular Fm operation, Bm operation is also possible, producing an intermittent beam at an accelerating frequency of 2,856 MHz divided by 64 or 128 (12). Details of the structure and features of LEBRA-FEL have been previously described (13-15). The Fm operating conditions in the present studies were an electron beam energy of about 80 MeV, a macro-pulse beam current of about 200 mA, a repetition frequency of 2.0 Hz, a macro-pulse width of about 20 μs, a micro-pulse width of about 1 ps, and a bunch interval of 350 ps. The Bm operating conditions were an electron beam energy of 80 MeV, a macro-pulse beam current of about 2.0 A, a repetition rate of 2.0 Hz, a macro-pulse width of about 20 μs, a micro-pulse width of about 1 ps, and a bunch interval of 22.4 ns. The FEL beam generated in the accelerator room is transported about 50 m in a vacuum duct, which is guided to the user's laboratory.

The wavelength of the FEL was adjusted to 2.94 μm, which is the same as that for Er:YAG lasers that are frequently used in clinical dentistry. The spot size and power for the FEL depend

on the wavelength. However, the inner diameter of the transport optics of the FEL beamline and the effective diameters of the mirrors and lenses of the irradiation optics limit the FEL spot size in the laboratory. The beam passes through a polarizing plate placed in the middle to fix the pulse energy. The spot diameter at that point was set to 25 mm, and the pulse energy was adjusted to 6.0 mJ/macro-pulse. The FEL beam was focused to several tens of micrometers using a calcium fluoride plano-convex lens with a diameter of 50 mm and a focal length of 100 mm. Since the FEL output varies between pulses, the laser power for each macro-pulse was monitored using a power meter during the experiments, and FEL irradiation was performed after confirming the mean value over a fixed duration of time. **Figure 3A** shows a schematic diagram of the electron beam pulse structures for Fm and Bm, and **Figure 3B** shows the LEBRA-FEL pulse structures.

Irradiation of LEBRA-FEL to the samples

The sectioned specimens were mounted on an automatic XYZ stage with a precision of 0.01 mm, and a computer program controlled the irradiation position. **Figure 4** shows photographs of the FEL optical system and a sample placed on the sample stage. The automated stage has been programmed to move 25 times every 1-mm step in the Y-direction. The stage was then offset in the X-direction by 1 mm, and the process was repeated in a raster-like pattern. In this study, each spot was irradiated with either 1 or 5 FEL macro-pulses, using either Fm or Bm.

The laser beam was focused on the sample surface at an incidence angle of 90° (normal incidence). The irradiation pattern is shown in **Figure 5**. In order to emulate a typical dental clinical environment, all irradiation experiments were performed at room temperature in the air.

Comparison of pit structures and depths after FEL irradiation

Observation of pits was performed using a stereomicroscope (SMZ1500, Nikon Corp., Tokyo, Japan), and all authors checked the shape and presence of scorch marks at full focus, and images were recorded using a digital camera. Measurements of the size and depth of pits were performed using a white-light interferometer-mounted laser microscope (VK-X3000, Keyence Corp., Osaka, Japan) capable of measuring surface profiles. The depth of the pit was measured at the deepest point, and the height of the bulge was automatically measured at the highest point by the laser scanning device.

Results

4-1. Formation of pits produced by LEBRA-FEL irradiation.

Figure 6 shows stereomicroscope images following LEBRA-FEL irradiation. The arrows indicate the locations where the pit formation was measured.

White turbidity and scorch marks that can be generated by Er:YAG lasers for dental clinical applications were not found in the enamel or dentin irradiated by LEBRA-FEL, regardless of the mode and number of pulse irradiations.

The pit depth was found to be shallow in enamel than in dentin. The pit diameter was about 150 μm for Fm and about 100 μm for Bm, regardless of the number of macro-pulses. Furthermore, all of the pits exhibited a conical shape. **Figure 7** shows 3D images of pits produced in Fm and Bm, captured from the inside of the surface profile with a laser microscope.

Although the pits in enamel and mantle-dentin were slightly deeper after single macro-pulse irradiation for Bm than for Fm. In another tooth site, Fm had a deeper Pit than Bm. However, as the number of macro-pulses irradiation increased, the pits became deeper for Fm than for Bm, regardless of the site on the tooth. The pit depth was proportionate to the number of macro-pulses irradiation. Furthermore, the bulge height was smaller for Bm than for Fm, regardless of the number of pulses irradiation.

A characteristic bulge was found around the pit in both the enamel and dentin following FEL irradiation. For Fm in particular, as the number of pulses increased, although the bulge tended

to be higher at the mantle and circumpulpal dentin, it was lower in the enamel and enamel-dentin junction. However, no large difference in bulge height was found for Bm regardless of the site on the tooth or the number of pulses. **Figure 8** shows a graph summarizing the pit depth and bulge height dependence on the number of FEL pulses for each irradiation mode.

Discussion

In this study, the LEBRA-FEL was used to irradiate human teeth in Fm and Bm modes.

When the surface of a solid material is irradiated with a laser pulse that exceeds the threshold fluence of the material, ablation (sputtering and peeling) occurs, creating marks on the surface. Although it is a simple phenomenon, many problems remain in terms of laser machining. This is because there are many parameters such as the environmental atmosphere and the type of material, in addition to the laser irradiation conditions (wavelength, pulse width, angle of incidence, beam diameter, spatial distribution, polarization, and the number of pulses). The development of laser technology has made a significant contribution to the field of medicine, and many laser-based treatments are applied in clinical dentistry (1). Recent lasers can produce pulses at repetition rates in the megahertz range, and the importance of understanding the interactions between the laser and the surface is increasing (16). Furthermore, it has been reported that the machining efficiency can be increased by selecting the irradiation mode (17).

In order to obtain the desired effect more efficiently when an object is irradiated by a laser beam, it is necessary to select the laser device based on the peak absorption wavelength for the components that make up the material being irradiated (18, 19). Furthermore, it has recently been reported that there is a dependence on the laser pulse width, even at the same wavelength (20).

The LEBRA-FEL is not only wavelength-tunable but also generates micro-pulses with pulse

widths of several hundred femtoseconds for both Fm and Bm. By varying the interval between micro-pulses at the same wavelength, useful information can be obtained on the pulse interval effect. For single macro-pulse irradiation, the pit depth was slightly larger in the enamel and mantle-dentin for Bm mode than for Fm. However, as the number of macro-pulses increased, the pits became deeper for Fm than for Bm, regardless of the site on the tooth. Initially, it was thought that deeper pits would be drilled with Bm, which has a higher power per micro-pulse. However, as the number of macro-pulses increased, deeper pits were observed for Fm than for Bm in both the enamel and the dentin. This suggests that differences in tooth pit formation occur when the pulse interval is short, even when the macro-pulse width is the same for both Fm and Bm. Typically, the power intensity per micro-pulse is much higher for Bm than for Fm, but the average intensity per macro-pulse is higher for Fm than for Bm. In the present study, a polarizing plate was inserted into the optical axis of the FEL to make the energy per macro-pulse uniform. Therefore, it is considered that deeper pits (stronger ablation) were formed using Fm with shorter pulse intervals as the number of micro-pulses increased.

The height of the bulge is slightly larger for Fm than for Bm, for both enamel and dentin. One reason for this is that the pulse interval for Fm is 350 ps while that for Bm is 22.4 ns, and the pulse interval for Fm is much shorter than that for Bm. Since heat is generated only at the position where the laser light is absorbed (21), the use of Fm with a narrower pulse interval causes molten tooth substance to accumulate around the pit, so that the bulge becomes higher.

The reason why the bulge height did not change in Bm no matter which part of the hard tissue of the tooth was irradiated may be because the number of micro-pulses was smaller compared to Fm, and the pulse interval was larger. Thus, ablation proceeded under conditions in which it was difficult for heat to accumulate in the tooth substance. It is also considered that in areas where there is little heat accumulation, ablation occurred with virtually no bulge formation by melting of tooth substance around the pit. When a tooth is irradiated by a laser with a pulse width shorter than the thermal relaxation time, heating occurs only at the position where the laser light is absorbed, and heat transfer does not occur to surrounding tissue, leading to no thermal effect (21). It was reported that pit formation in a tooth during LEBRA-FEL irradiation in Fm was due to a type of plasma evaporation and not processes such as thermal evaporation (10, 22). In the present study, since the amount of irradiation energy in Fm and Bm are on the order of sub-Tera-watts to Tera-watts per centimeter squared per micro-pulse, such plasma evaporation is thought to have occurred on the tooth structure.

As described above, the laser used in the present study has a pulse width of several hundred femtoseconds, and the ablation efficiency for the same average power is expected to be much lower than that for microsecond or nanosecond laser pulses (23). As a result, for the same average power, it is necessary to increase the number of pulse irradiations in order to achieve sufficient processing. On the other hand, because of the narrow micro-pulse width for LEBRA-FEL, thermal conduction to the area around the irradiated site can be ignored, similar to the

case for femtosecond laser ablation (24, 25). Furthermore, the shortest thermal relaxation time exhibited by water at a wavelength of 2.94 μm is around 1 μs (21, 26). Because of this, since the FEL used in the present study has a micro-pulse width sufficiently shorter than the thermal relaxation time for water, the tooth substance is ablated before thermal conduction occurs. This suggests that it is possible for pits to form without visible scorch marks, even without water injection.

In clinical dentistry, it is extremely useful to perform drilling without heat or scorch marks appearing on teeth, and subsequent restorative operations can be easily performed with excellent results. The conventional laser light that is currently used in clinical dentistry has a restricted range of wavelengths and pulse widths so its application to research is limited. Since FEL pulses consist of high-power micro-pulse with femtosecond pulse widths, it is a useful tool for fundamental research aimed at optimizing radiation parameters and determining interaction mechanisms between tooth hard tissues and laser beams, beyond what is possible using conventional lasers. In the future, it is anticipated that this will assist with the development of safer dental lasers.

In conclusion, as the number of macro-pulse irradiations increased, the pits became deeper in Fm than in Bm, regardless of the site on the tooth. On the other hand, the bulge height was lower for Bm than for Fm, regardless of the site on the tooth or the number of macro-pulse irradiations. No scorch marks were observed in the pits for either mode. These were found to

be due to differences in micro-pulse intervals within the macro-pulse structures of Fm and Bm. The intensity of the FEL irradiation caused plasma evaporation in the tooth hard tissue, and the tooth substance was ablated before thermal conduction occurred. The relation with the thermal relaxation time also confirmed that pits were formed without visible scorch marks, even without water injection. High-power micro-pulses with femtosecond micro-pulse widths in the pulse structure were shown to be useful in the development of dental lasers.

Acknowledgments

The FEL used in the present study was a device managed by the Institute of Quantum Science and Technology of Nihon University (located on the Funabashi campus of the College of Science and Technology of Nihon University).

The LEBRA project was designed by the late Prof. Isamu Sato, who moved from the High Energy Accelerator Research Organization (KEK) and was started in 2000. The authors thank Prof. Hayakawa. Y, Dr. Hayakawa. K, and Dr. Nogami. K for cooperating in this FEL study. The Authors also thank the LEBRA members for allowing us to use their equipment. In addition, the authors would like to thank prof. Okada. H, prof. Kaneda, T., and prof. Kondo. S, who instructed them in this research. Part of this study was conducted by the "Joint Usage/Research Program on Zero-Emission Energy Research, Institute of Advanced Energy, Kyoto University (ZE2022C-11).

Conflict of Interests: The authors declare that no conflicts of interests exist.

References

1. Kono T, Sakae T, Sakai T, Zen H, Ohgaki H, Hayakawa Y, Okada H: Application of free electron laser in dentistry; From research in LEBRA-FEL and KU-FEL. JJLPS, 29: 166-171, 2022.
2. Sharma N, Williams C, Angadi P, Jethlia H: Application of lasers in dentistry. Res Rev J Dent Sci, 1:22–25, 2013.
3. Tsuchida T: Laser treatments in the current medical fee revision 2022. JJSLSM, 43: 30-58, 2022. (in Japanese)
4. Einstein A: "Zur quantentheorie der strahlung," physik. Zeits, 18: 121-128, 1917.
5. Maiman TH: Stimulated optical radiation in ruby. Nature, 187: 493-494, 1960.
6. Goldman L, Hornby P, Meyer R, Goldman B: Impact of the LASER on dental caries. Nature, 203: 417, 1964.
7. Ishikawa I, Aoki A, Takasaki AA, Mizutani K, Sasaki KM, Izumi Y: Application of lasers in periodontics: true innovation or myth? Periodontol 2000, 50: 90-126, 2009.
8. McNeil BWJ, Thompson NR: X-ray free-electron lasers. Nature Photon, 4: 814–821, 2010.
9. Heya M, Fukami Y, Awazu K: Status and prospects of mid-IR pulsed-laser researches in molecule-vibration region for bio-molecule surgery. Jpn J Opt, 30: 667-672, 2001. (in Japanese)
10. Sakae T, Sato Y, Tanimoto Y, Higa M, Oinuma H, Kozawa Y, Okada H, Yamamoto H,

Hayakawa T, Nemoto K, Sakai T, Nogami K, Mori A, Kuwada T, Hayakawa Y, Tanaka T, Hayakawa K, Sato I: Pit formation in human enamel and dentin irradiated using the 2.94 μm LEBRA-free electron laser. Int J Oral-Med Sci, 4: 8-13, 2005.

11. Sakae T, Sato Y, Okada H, Yamamoto H, Tanimoto Y, Hayakawa T, Hayakawa Y, Hayakawa K, Tanaka T, Sato I: Wavelength dependency and plasma ablation of free electron laser irradiation to dental hard tissues. JJSLSM, 29: 106-111, 2008. (in Japanese)
12. Sakai T: Development and application of electron linac at LEBRA in Nihon University. J JSSRR, 34: 153-162, 2021. (in Japanese)
13. Tanaka T, Hayakawa K, Hayakawa Y, Mori A, Nogami K, Sato I, Yokoyama K: Tunability and power characteristics of the LEBRA infrared FEL, In: Bakker R, Walker R, editors. FEL2004 26th International Free-Electron Laser Conference and 11th FEL User-Workshop, Trieste: Sincrotrone Trieste (ELETTRA); 2004, p. 247-250.
14. Nakao K, Hayakawa K, Hayakawa Y, Inagaki M, Nogami K, Sakai T, Tanaka T: Pulse structure measurement of near-infrared FEL in burst-mode operation of LEBRA linac. In: Shintake T, editor. FEL2012 34th International Free-Electron Laser Conference, Nara: Spring-8; 2012, p. 472‑474, 2012.
15. Tanaka T: Development of wideband coupled undulator at LEBRA. http://www.lebra.nihon-u.ac.jp/pdf/ws/2undul.pdf. (in Japanese) (Accessed 2022-11-22)
16. Hashida M, Furukawa Y, Masuno S, Takenaka K, Tsukamoto M: Ablation suppression with

double pulsed femtosecond laser beam. JJLPS, 29: 131-135, 2022. (in Japanese)

17. Kerse C, Kalaycıoğlu H, Elahi P, Çetin B, Kesim DK, Akçaalan Ö, Yavaş S, Aşık MD, Öktem B, Hoogland H, Holzwarth R, Ilday FÖ: Ablation-cooled material removal with ultrafast bursts of pulses. Nature, 537: 84‑88, 2016.
18. Arrastia AMA, Machida T, Matsumoto K: A comparative thermometric study of four semiconductor laser devices, J Showa Univ Soc, 11: 362-366, 1991.
19. Niemz MH: Cavity preparation with the Nd:YLF picosecond laser, J Dent Res, 74: 1194-1199, 1995.
20. Uchizono T, Igarashi A, Kato J, Hirai Y, Mohri D, Awazu K: Histological observation on dental hard tissue irradiated by ultra-short pulsed laser, J Jpn Soc Laser Dent, 17: 81-86, 2006. (in Japanese)
21. Heya M, Ucchizono T, Aawazu K, Basic interactions of dental hard tissue with laser. JJSLSM, 25: 323−331, 2005. (in Japanese)
22. Sakae T, Sato Y, Numata Y, Suwa T, Hayakawa T, Suzuki K, Kuwata T, Hayakawa K, Hayakawa Y, Tanaka T, Sato I: Thermal ablation of FEL irradiation using gypsum as an indicator; Lasers Med Sci, 22: 15−20, 2007.
23. Kusunose TK, Kusunose A, Wakami M, Takebayashi C, Goto H, Aida M, Sakai T, Nakao K, Nogami K, Inagaki M, Hayakawa K, Suzuki K, Sakae T: Evaluation of irradiation effects of near-infrared free-electron-laser of silver alloy for dental application. Lasers Med Sci, 32:

1349–1355, 2017.

24. Chichkov BN, Momma C, Nolte S, Alvensleben F, Tünnermann A: Femtosecond, picosecond and nanosecond laser ablation of solids. Appl Phys A, 63: 109–115, 1996.

25. Leitz KH, Redlingshöfer B, Reg Y, Otto A, Schmidt M: Metal ablation with short and ultrashort laser pulses. Phys Procedia, 12: 230–238, 2011.

26. Fried D, Zuerlein M, Featherstone JDB, Seka W, Duhn C, McCormack SM: IR laser ablation of dental enamel: mechanistic dependence on the primary absorber. Appl Surf Sci, 127-129: 852-856, 1998.

Table 1 Specifications of LEBRA 125 MeV electron linac

Acceleration frequency	2,856 MHz
Beam energy	40~ 100 MeV (typ.)
DC electron gun energy	100 kV
Klystron peak RF power	~20 MW
Number of klystrons	2
Macro-pulse width	5~ 20 μs
Macro-pulse repetition rate	2~ 10 pps
Macro-pulse beam current	200 mA~ 2 A
Energy spread (FWHM)	0.5~ 1 %

Figures and Legends

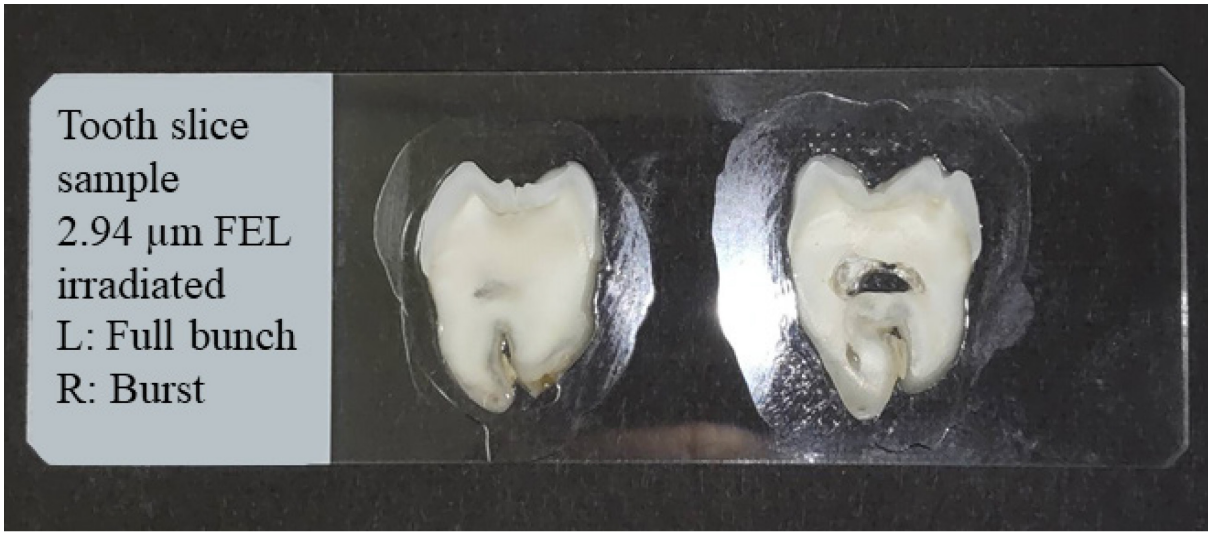

Figure 1 Photograph of tooth sliced to 0.5 mm and attached to the glass slide.

The teeth were cut in longitudinally parallel to the buccolingual tooth axis. Sliced sections were used as samples with a thickness of approximately 0.5 mm and polished. Slices of the same tooth were attached to a single glass slide.

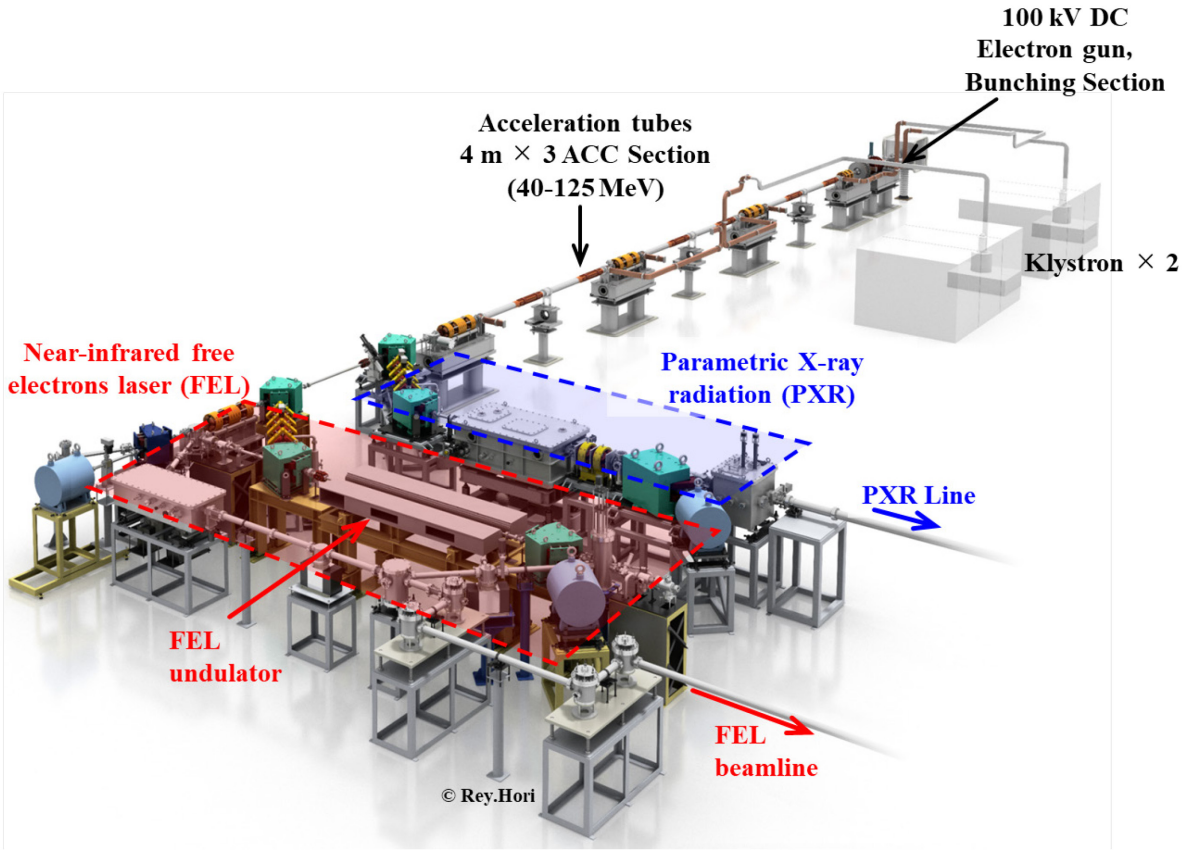

Figure 2 Each beamline in the LEBRA accelerator room.

The DC electron gun generates a full bunch mode or burst mode electron beam, and the FEL undulator defines the wavelength of the FEL.

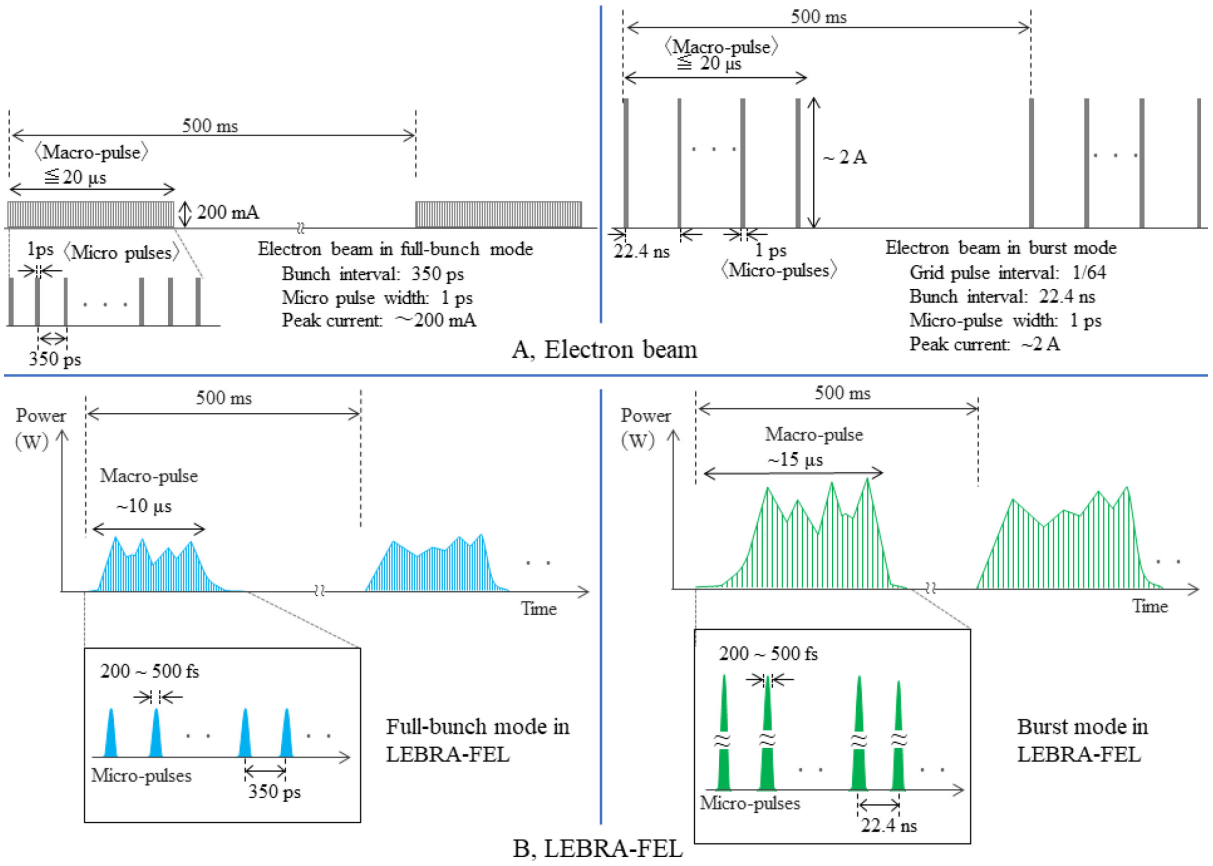

Figure 3 Time structure for full bunch mode and burst mode in LEBRA

A, Time structure of electron beam.

B, Time structure of LEBRA-FEL beam.

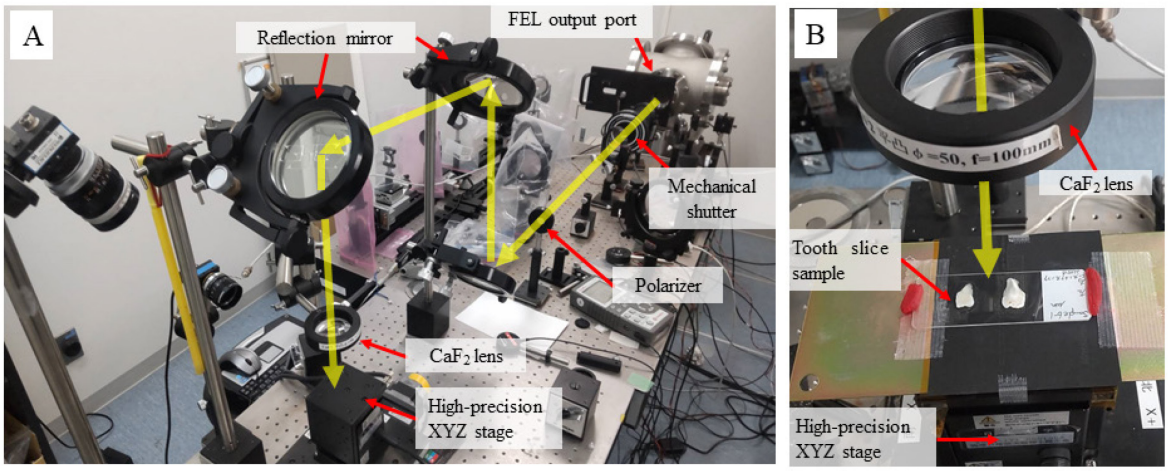

Figure 4 Irradiation equipment in FEL laboratory.

The FEL beam passes along a vacuum tube from the CaF_2 windows at the rear side (A). Yellow arrows indicate the optical axis of the FEL beam. The beam passes through a polarizer and three reflectors and then enters the condenser lens (CaF_2, f = 100 mm) and is focused on the sample surface (B).

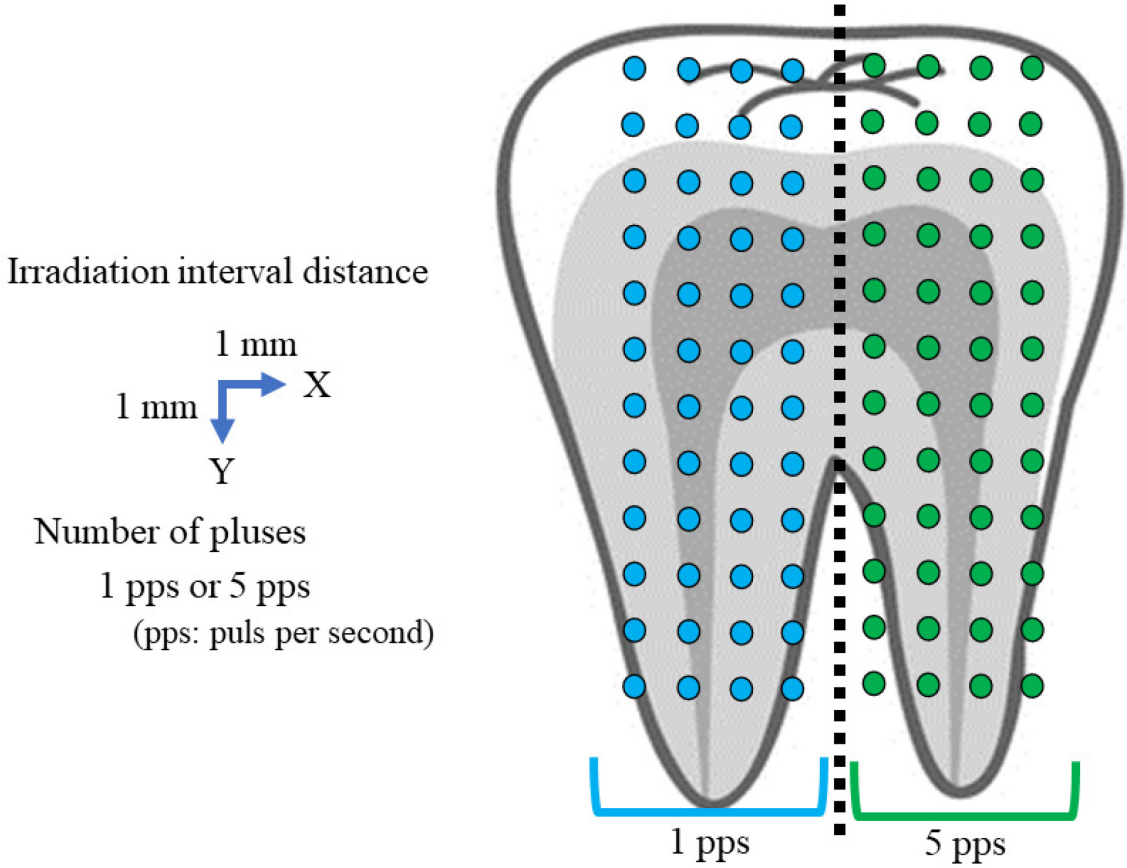

Figure 5 Schematic diagram of full-bunch mode and burst mode irradiation at a wavelength of 2.94 μm.

The automated stage has been programmed to move 25 times every 1-mm step in the Y-direction. The stage was then offset in the X-direction by 1 mm, and the process was repeated in a raster-like pattern.

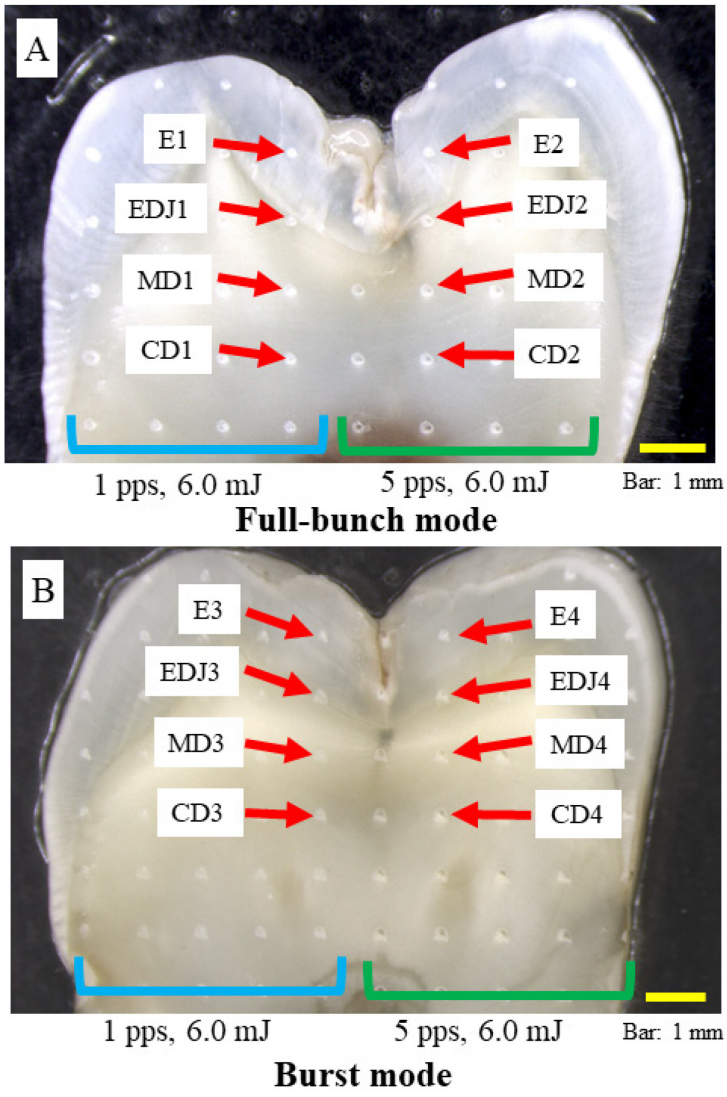

Figure 6 Stereomicroscopic image after FEL irradiation.

The red arrows in each photo indicate the area where the pit formation was measured.

E: Enamel, EDJ: Enamel-dentin junction, MD: Mantle-dentin,

CD: Circumpulpal dentin

A, FEL irradiation at a wavelength of 2.94 μm in full-bunch mode.

B, FEL irradiation at a wavelength of 2.94 μm in burst mode.

In both figures, the blue frame shows 1 pulse of 6.0 mJ FEL irradiation, and the green frame shows 5 pulses.

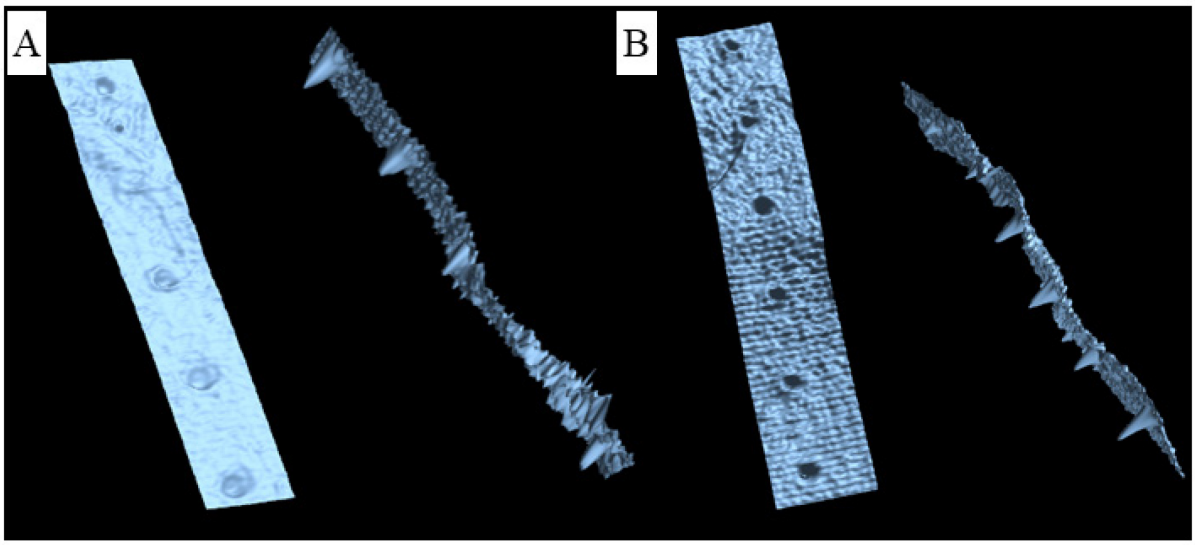

Figure 7 Surface magnified 3D image of pit formation.

3D image of the pit formations captured from the inside of the surface profile with a laser microscope. Both images are for a single FEL pulse at a wavelength of 2.94 μm with 6.0 mJ/ macro-pulse.

The pit diameter was about 150 μm for Fm and about 100 μm for Bm. Furthermore, all the pits exhibited a conical shape.

A, Full-bunch mode.

B, Burst mode.

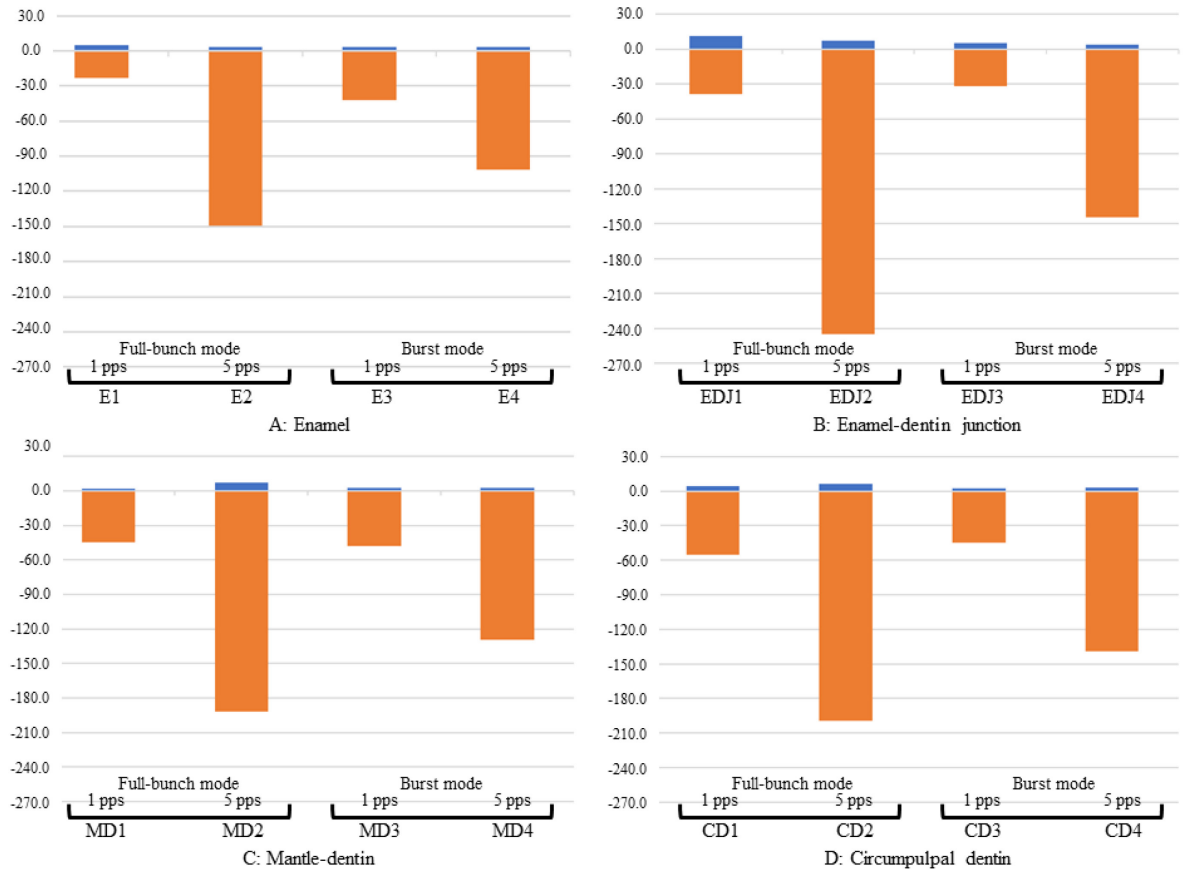

Figure 8 Dependence of pit depth and bulge height on the number of pulses for each FEL mode.

The horizontal axis corresponds to the FEL irradiation points in Figure 6. The orange vertical bars represent the pit depth, and the blue vertical bars indicate the bulge height around the pit. Vertical axis scale: μm.

A, Enamel

B, Enamel-dentin junction

C, Mantle-dentin

D, Circumpulpal dentin.